frontiers in Energy Research

MINI REVIEW
published: 17 June 2020
doi: 10.3389/fenrg.2020.00097

Effective Approaches of Improving the Performance of Chalcogenide Solid Electrolytes for All-Solid-State Sodium-Ion Batteries

Hanqing Dai[1], Wenqian Xu[2], Zhe Hu[3], Yuanyuan Chen[3], Xian Wei[3], Bobo Yang[1], Zhihao Chen[1], Jing Gu[2], Dan Yang[3], Fengxian Xie[3], Wanlu Zhang[3], Ruiqian Guo[1,3], Guoqi Zhang[1,4,5]* and Wei Wei[2]**

[1] Academy for Engineering and Technology, Institute of Future Lighting, Fudan University, Shanghai, China, [2] College of Electronic and Optical Engineering, Nanjing University of Posts and Telecommunications, Nanjing, China, [3] Engineering Research Center of Advanced Lighting Technology, Ministry of Education, Fudan University, Shanghai, China, [4] Shenzhen Institute of Wide-Bandgap Semiconductors, South University of Science and Technology, Shenzhen, China, [5] Department of Microelectronics, Delft University of Technology, Delft, Netherlands

OPEN ACCESS

Edited by:
Guang Yang,
Oak Ridge National Laboratory (DOE), United States

Reviewed by:
Wen Luo,
Wuhan University of Technology, China
Chun Fang,
Huazhong University of Science and Technology, China

***Correspondence:**
Ruiqian Guo
rqguo@fudan.edu.cn
Guoqi Zhang
G.Q.zhang@tudelft.nl
Wei Wei
weiwei@njupt.edu.cn

Specialty section:
This article was submitted to Electrochemical Energy Conversion and Storage, a section of the journal Frontiers in Energy Research

Received: 04 March 2020
Accepted: 05 May 2020
Published: 17 June 2020

Citation:
Dai H, Xu W, Hu Z, Chen Y, Wei X, Yang B, Chen Z, Gu J, Yang D, Xie F, Zhang W, Guo R, Zhang G and Wei W (2020) Effective Approaches of Improving the Performance of Chalcogenide Solid Electrolytes for All-Solid-State Sodium-Ion Batteries. Front. Energy Res. 8:97. doi: 10.3389/fenrg.2020.00097

All-solid-state sodium-ion batteries (SIBs) possess the advantages of rich resources, low price, and high security, which are one of the best alternatives for large-scale energy storage systems in the future. Also, the chalcogenide solid electrolytes (CSEs) of SIBs have the characteristics of excellent room-temperature ionic conductivity (10^{-3}-10^{-2} S cm^{-1}), low activation energy (<0.6 eV), easy cold-pressing consolidation, etc. Hence, CSEs have become a very active area of all-solid-state SIB research in recent years. In this review, the modification methods and implementation technologies of CSEs are summarized, and the structure and electrochemical performance of the CSEs are discussed. Furthermore, the auxiliary function of first-principle calculations for modification is introduced. Ultimately, we describe the challenges regarding CSEs and propose some strategic suggestions.

Keywords: chalcogenide solid electrolytes, modification methods, first-principle calculations, electrochemical performance, sodium-ion batter

INTRODUCTION

Recently, due to the rapidly amplified demand for electric vehicles and power storage systems based on renewable energy, the development of large-scale energy storage systems (ESSs) has aroused the attention of the whole world (Zhong et al., 2014; Dai et al., 2020; Yao et al., 2020). Considering safety and cost of large-scale ESSs, all-solid-state sodium-ion batteries (SIBs) could be an alternative to all-solid-state lithium ion batteries (LIB) (Luo et al., 2016). Additionally, compared with liquid electrolytes, solid electrolytes possess the leak-free state, wide electrochemical windows, and high thermal stability over a broad temperature range (Wang et al., 2019a). Therefore, the development of solid electrolytes is a very meaningful task.

Generally, solid electrolytes can be divided into three main categories: organic solid electrolytes, composite solid electrolytes, and inorganic solid electrolytes (Hou et al., 2018; Krauskopf et al., 2018a; Zhao et al., 2018; Kobayashi et al., 2020). Moreover, inorganic solid electrolytes include Na-β-Al_2O_3, NASICON (Na super ionic conductor), borohydride, and chalcogenide. At present, chalcogenide solid electrolytes (CSEs) are mainly divided into four categories: Na_3MS_4

(M = P, Sb) series (Tanibata et al., 2017; Krauskopf et al., 2018a; Noi et al., 2018; Takeuchi et al., 2018; Zhao et al., 2018; Zhang et al., 2020), Na_3MSe_4 (M = P, Sb) series (Bo et al., 2016; Mahmoud et al., 2019), $Na_mM_xP_yX_{12}$ (M = Si, Ge, Sn; X = S, Se; $10 \leq m \leq 11$; x/y = 1/2 or 2) series (Kato et al., 2016; Richards et al., 2016; Wan et al., 2020), and $Na_7P_3X_{11}$ (X = O, S, Se) series (Wang et al., 2017). The most common in the Na_3MS_4 (M = P, Sb) series is Na_3PS_4, which has two crystal forms: tetragonal (P −4 21 c; a = b = 0.69520 nm, c = 0.70757 nm) and cubic (I −4 3 m; a = b = c = 0.70699 nm) (Tanibata et al., 2017; Krauskopf et al., 2018a; Takeuchi et al., 2018; Zhao et al., 2018). The room-temperature (RT) conductivity of glass ceramic Na_3PS_4 (10^{-4} S cm^{-1}, RT) is higher than that of glass (10^{-5} S cm^{-1}, RT), and that of tetragonal Na_3PS_4 (t-Na_3PS_4, 10^{-3} S cm^{-1}, RT) is higher than that of cubic Na_3PS_4 (c-Na_3PS_4, 10^{-5} S cm^{-1}, RT). Moreover, first-principle calculations (FPCs) show that the conduction of sodium ions in c-Na_3PS_4 and t-Na_3PS_4 is similar (Krauskopf et al., 2018a). For the Na_3MSe_4 (M = P, Sb) series, FPCs indicate that defects are the key to the conduction of sodium ions in cubic Na_3MSe_4 (Bo et al., 2016), including Na vacancy, interstitial Na, and Frenkel defect. Among these defects, the Na vacancy formation energy is the lowest, which is the main mechanism to improve the conduction of sodium ions. As for the $Na_mM_xP_yX_{12}$ (M = Si, Ge, Sn; X = S, Se; $10 \leq m \leq 11$; x/y = 1/2 or 2) series (Kato et al., 2016; Rao et al., 2017), their crystal structure is similar to $Li_{10}GeP_2S_{12}$. Generally, NaM_6 octahedron forms a 3D transmission network via coplanarity, which enables sodium ion to conduct rapidly (Kato et al., 2016). In terms of the $Na_7P_3X_{11}$ (X = S, Se) series, FPCs demonstrates that the RT ionic conductivities of $Na_7P_3S_{11}$ and $Na_7P_3Se_{11}$ are higher than 10 mS cm^{-1}, respectively (Wang et al., 2017). However, the polarizability of oxygen is weaker than that of sulfur and selenium, and the distance between Na^+ and P^{5+} ions of $Na_7P_3O_{11}$ is shorter than that of $Na_7P_3S_{11}$ and $Na_7P_3Se_{11}$. Therefore, the stronger interaction between cations results in the larger change of Na site energy and the higher activation energy required for Na^+ migration in $Na_7P_3O_{11}$. Therefore, the RT ionic conductivity of $Na_7P_3O_{11}$ is only 0.003 mS cm^{-1}.

Since the electronegativity of sulfur is lower than that of oxygen, sulfide electrolytes usually exhibit faster sodium ion conduction than oxide electrolytes because the electrostatic force of sulfur and sodium ion is less than that of oxygen and sodium ion. Compared with oxide solid electrolyte, chalcogenide solid electrolytes (CSEs) could be synthesized at low temperature, which reduces the production cost. Due to the deformability of CSEs, it can achieve good interface contact with electrode interface via simple cold pressing to further reduce the actual production cost. Nay, CSEs have high RT ionic conductivity and low activation energy. Among all kinds of solid electrolytes, CSEs with good formability are a good choice for the preparation of bulk-type all-solid-state SIBs. Therefore, CSEs have an important application prospect in the field of bulk-type all-solid-state SIBs for large-scale energy storage. Despite these advantages, there are still some challenges before CSEs are widely used. Initially, the composite electrodes of bulk-type all-solid-state SIBs are in poor contact. Although CSEs have deformability, investigation results demonstrate cold pressing alone is not enough to form compact components without voids. Secondly, CSEs are unstable in the air, which are easy to deliquesce, oxidize, and generate toxic gases, resulting in a sharp drop of conductivity. Therefore, it is very important to improve the performance of CSEs in bulk-type all-solid-state SIBs.

This review will introduce the CSEs from the following aspects: the modification methods and the implementation technologies, the structure and electrochemical performance, and the auxiliary function of FPCs for modification. Ultimately, we describe the challenges of the CSEs and propose some strategic suggestions.

IMPROVING APPROACHES OF THE CSEs

For the CSEs, especially chalcogenide glass-ceramic electrolytes, they not only have high room-temperature ionic conductivity ($10^{-3} > \sigma > 10^{-5}$ S cm^{-1}) but also have a wide electrochemical window (V_{EW}, 6 V> V_{EW} > 4 V) and suitable mechanical properties (Hayashi et al., 2012; Kim et al., 2014; Tanibata et al., 2014a). In recent years, to more effectively enhance the electrochemical properties and mechanical properties of the CSEs, the following effective methods are used in the developments: ion doping and substitution, composite method, crystal transformation method, ceramization, and vitrification, etc. In this section, the effect of modification of different methods on the CSEs is compared vertically, mainly from the aspects of electrochemical window, ionic conductivity, and electrical stability as well as structural stability.

Ion Doping and Substitution

Ion doping and substitution are common methods of material modification (Bo et al., 2016; Kato et al., 2016; Richards et al., 2016; Krauskopf et al., 2017; Rao et al., 2017; Wang et al., 2017; Mahmoud et al., 2019; Wan et al., 2020; Zhang et al., 2020). Cation ion doping into the P site or halogen doping into the S site can introduce vacancies to improve the ionic conductivity of the CSEs (Zhang et al., 2015; Bo et al., 2016; Wang et al., 2016; Krauskopf et al., 2017, 2018a,b; Yu et al., 2017). The bond energy between ions and adjacent atoms could be changed by ion doping and substitution to improve the ionic conductivity of the electrolyte (Krauskopf et al., 2018a). Furthermore, the diffusion activation energy of ions can be further changed by this method (Bo et al., 2016; Krauskopf et al., 2017). Additionally, ion doping and substitution not only introduce vacancy but also play an important role in micro diffusion (Yu et al., 2017; Krauskopf et al., 2018b). After doping and substitution, the free volume caused by phonon is large, and the transition probability of sodium ion from one site to the adjacent site is increased. For example, the ionic conductivity of Sb^{5+} instead of P^{5+} or Se^{2-} instead of S^{2-} in Na_3PS_4 has been improved markedly (Zhang et al., 2015; Bo et al., 2016; Wang et al., 2016). Similarly, $Na_3P_{0.62}As_{0.38}S_4$ with the replacement of P^{5+} to As^{5+} was developed with an exceptionally high room-temperature ionic conductivity of 1.46×10^{-3} S cm^{-1} and enhanced moisture stability (Yu et al., 2017). Peradventure, Cl^{-1} instead of S^{2-} in Na_3PS_4 was obtained by a liquid-phase (suspension) method,

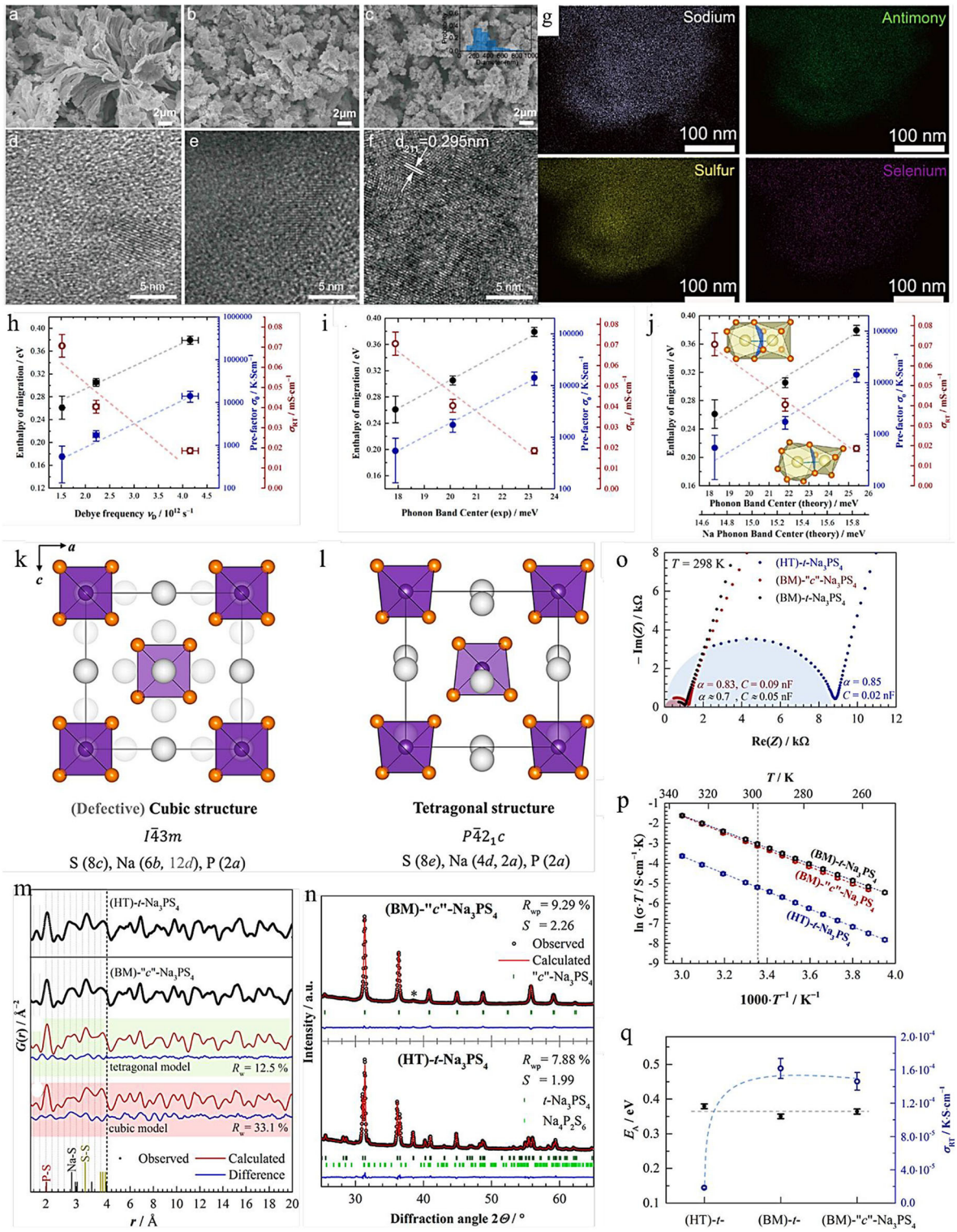

FIGURE 1 | SEM images of $Na_3SbS_{3.75}Se_{0.25}$ electrolytes synthesized by **(a)** liquid-phase method, **(b)** solid-phase method, and **(c)** liquid/solid fusion technology (the inset is the statistical particle size distribution of the electrolytes). HRTEM images of $Na_3SbS_{3.75}Se_{0.25}$ electrolytes synthesized by **(d)** liquid-phase method, **(e)** solid-phase method, and **(f)** liquid/solid fusion technology. **(g)** STEM images of $Na_3SbS_{3.75}Se_{0.25}$ electrolytes synthesized liquid/solid fusion technology (source Wan et al., 2019). Reproduced by permission of Elsevier B.V. https://doi.org/10.1016/j.nanoen.2019.104109. Correlation between measured enthalpy of migration E_A and prefatory σ_0 and **(h)** the measured Debye frequency, **(i)** the measured (total) phonon band center, and **(j)** the computed total and Na-projected

(Continued)

FIGURE 1 | band center (source: Krauskopf et al., 2018a). Reproduced by permission of American Chemical Society https://doi.org/10.1021/jacs.8b09340 Crystal structure of **(k)** c-Na_3PS_4 and **(l)** t-Na_3PS_4. **(m)** Experimental G(r) data for HT-t-Na_3PS_4 and BM-c-Na_3PS_4. **(n)** Rietveld refinements of XRD for (BM)-c-Na_3PS_4 and HT-t-Na_3PS_4. **(o)** Nyquist plots of t-Na_3PS_4 and c-Na_3PS_4 at different synthetic approaches. **(p)** Arrhenius plots of all compounds. **(q)** Activation energy and room-temperature ionic conductivity for different types of Na_3PS_4 (source Krauskopf et al., 2018a). Reproduced by permission of American Chemical Society https://doi.org/10.1021/acs.inorgchem.8b00458.

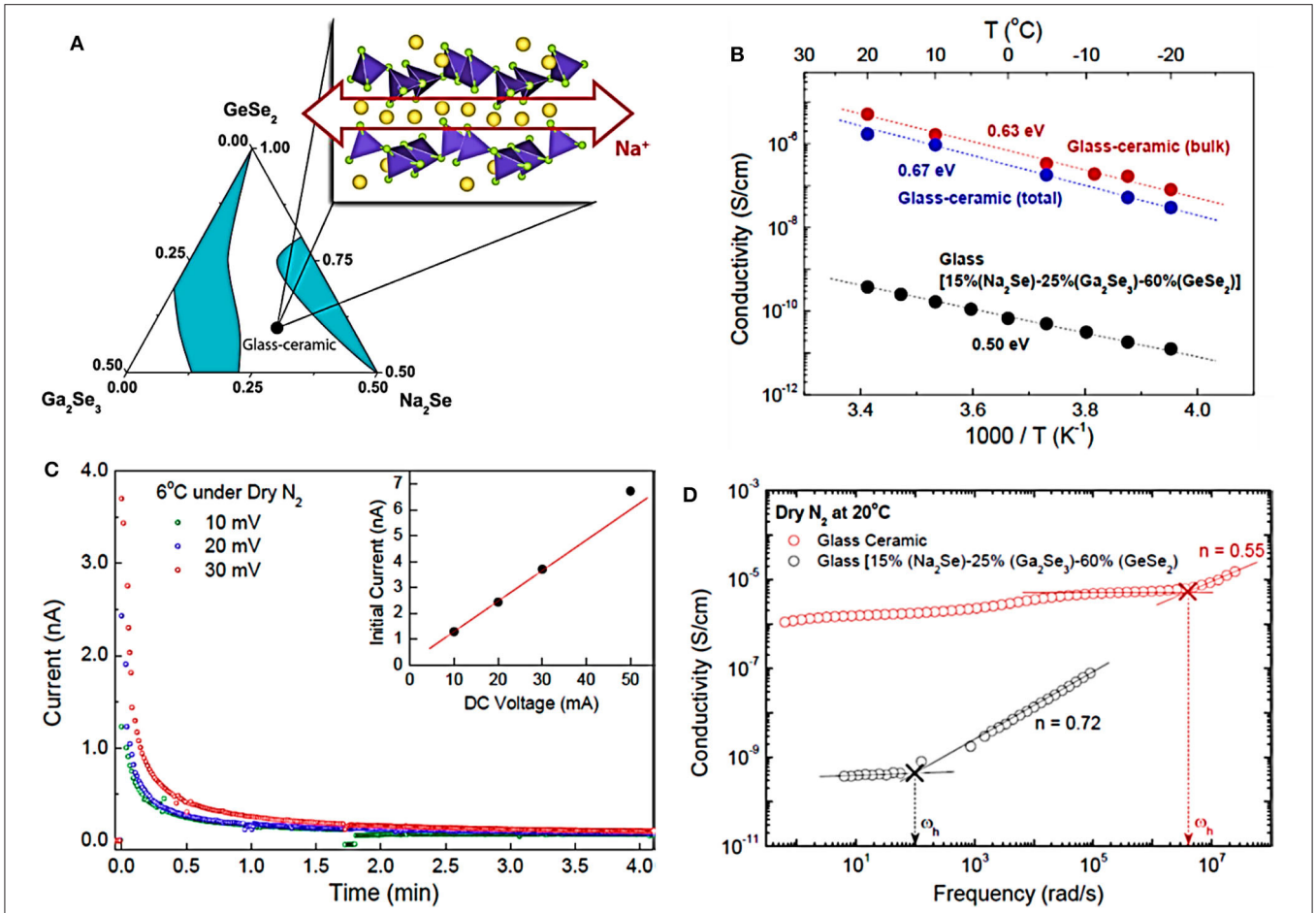

FIGURE 2 | (A) Ternary phase diagram of glass and glass ceramics. **(B)** Arrhenius plots of both the bulk and the total conductivities of the glass-ceramic and the glass materials. **(C)** Curves of the glass-ceramic material. **(D)** Bode plots of AC impedance spectra of the glass-ceramic and the glass materials at 20°C. The arrows reveal the frequency hopping signal of Na^+ in the two samples (source: Kim et al., 2014). Reproduced by permission of American Chemical Society https://doi.org/10.1021/cm502542p.

such as $Na_{2.9375}PS_{3.9375}Cl_{0.0625}$ with high room-temperature ionic conductivity of 4.3×10^{-4} S cm^{-1} (Uematsu et al., 2019).

Here, we choose one of the most representative examples to exhibit the effect of ion doping and substitution at the same time. The cubic $Na_3PS_{4-x}Se_x$ (c-$Na_3PS_{4-x}Se_x$) materials were developed by the mechanochemical (BM) approach and high temperature (HT), respectively (Krauskopf et al., 2017). The FPCs illustrate that the replacement S with Se could not only expand the diffusion path but also enhance the ionic conductivity. Recently, Yao et al. synthesized the $Na_3SbS_{3.75}Se_{0.25}$ solid electrolyte with less grain-boundary resistance by a liquid/solid fusion technology, as shown in **Figures 1a–g**. The $Na_3SbS_{3.75}Se_{0.25}$ solid electrolyte shows a high RT ionic conductivity of 4.03×10^{-3} S cm^{-1} owing to the significantly decreased amorphous phase in the electrolyte, and the small particle size of the solid electrolytes enhances the contact between solid electrolyte and electrode, reducing the interfacial contact resistance (Wan et al., 2019).

Additionally, Krauskopf et al. had investigated the lattice dynamics of the superionic conductor $Na_3PS_{4-x}Se_x$ by probing the optical phonon modes and the acoustic phonon modes, as well as the phonon density of states via inelastic neutron scattering, as shown in **Figures 1h–j** (Krauskopf et al., 2018b). The experimental results and FPCs have proved the influence of lattice dynamics and the softness of lattice to ion transport. When studying the change of the phonon spectrum or the density of

state of the total phonon, they observed the activation barrier of migration and the decrease in migration entropy and emphasized that the paradigm of "the softer the lattice, the better" is not always true. Additionally, ion doping and substitution can also improve the specific capacity of the battery. Although this change enhances the ionic conductivity and charge/discharge-specific capacity, it does not significantly change the electrochemical window of the electrolyte. In addition, owing to the excessive embedment of sodium ions in the electrolyte, this method will lead to the destruction of the electrolyte structure.

Composite Method

In terms of inorganic–organic composite, due to the strong ability of dissolving sodium salt in the amorphous region of polyethylene oxide (PEO), the PEO-based composite solid electrolyte is considered as an ideal solid electrolyte. The addition of inorganic materials reduces the crystallinity of the polymer matrix and improves the activity of the polymer chain. The addition of inorganic compounds to the polymer acts as a plasticizer, which is conducive to the transition of the polymer to an amorphous structure that is easy to transport ions. Moreover, the existence of active crystal and polymer can make the composite solid electrolyte have relatively high ionic conductivity, good flexibility, stability, and interface compatibility with sodium anode.

Recently, a typical inorganic–organic composite CSE of Na_3PS_4-PEO for all-solid-state SIB was obtained by the solution-phase reaction method with room-temperature ionic conductivity of 9.4×10^{-5} S cm^{-1} and electrochemical window of ∼4.5 V (Xu et al., 2020). Moreover, the PEO coating on the surface of Na_3PS_4 particles effectively hinders the side reaction between electrolyte and sodium metal electrode. After 40 cycles, the specific capacity of all-solid-state SIB is 230 mAh g^{-1}. Additionally, the $Na_{3-x}PS_{4-x}Cl_x$-PEO-$NaClO_4$ solid electrolyte with room-temperature ionic conductivity of 8.75×10^{-4} S cm^{-1} was obtained by the heat treatment (Wang et al., 2019b).

However, inorganic–inorganic composite materials are rare, mainly related to glass ceramic electrolytes. For example, $Na_3Zr_2Si_2PO_{12}$-Na_3PS_4 glass ceramics exhibited high total conductivities of 1.1×10^{-3} at 100°C; the results suggest that the composite materials make the contact between particles closer, which is conducive to the improvement of ionic conductivity (Noi et al., 2018). Similarly, for the sulfide-based solid electrolyte Na_3SbS_4-Na_2WS_4 with RT ionic conductivity of 4.28 mS cm^{-1} prepared by the liquid phase method, they point out that the increase in ionic conductivity is caused by sodium vacancies (Yubuchi et al., 2020).

Crystal Transformation Method

High-temperature heat treatment, ion doping, and substitution are widely applied in crystal transformation. The essence of crystal phase transition is that the crystal structure changes at a temperature higher than its phase transition temperature, while the reason for the phase transition caused by doping and substitution is that its process includes high-temperature treatment steps. The experimental results indicate that the tetragonal structure is stable at low temperature, while the cubic structure is more stable at high temperature (Hayashi et al., 2012). As we know, Na_3PS_4 crystallizes in one of two different polymorphs (i.e., cubic or tetragonal). FPCs of the cubic and tetragonal Na_3PS_4 (c-Na_3PS_4 and t-Na_3PS_4) are illustrated in **Figure 1** (Zhao et al., 2018).

The results reveal that both c-Na_3PS_4 and t-Na_3PS_4 are highly conductive solid electrolytes (De Klerk and Wagemaker, 2016). Although t-Na_3PS_4 exhibits higher ionic conductivity than c-Na_3PS_4 (Zhao et al., 2018), the ionic conductivity of c-Na_3PS_4 formed by ion doping and substitution method is higher than that of t-Na_3PS_4 (Zhu et al., 2015). Moreover, for the $Na_3PS_{4-x}Se_x$ materials, it is found that ion doping could be adopted to modify the crystal type due to its process which includes high-temperature treatment steps. Analogously, although RT ionic conductivity of tetragonal Na_3SbS_4 is high at 3 mS cm^{-1}, both experiments and theoretical calculations illustrate that the ionic conductivity of cubic Na_3SbS_4 is higher than that of tetragonal Na_3SbS_4 (Zhang et al., 2016, 2018).

Ceramization and Vitrification

Ceramization and vitrification is also a common approach to modify the solid electrolyte (Tanibata et al., 2014b; Park et al., 2018; Tsuji et al., 2018; Ma et al., 2020). Vitrification is the process of transforming a substance into the glassy state, in which there is no crystal structure. However, there are crystal phases in the ceramics after ceramization. Glass ceramic is a mixture of crystalline phase and residual glass phase, which is formed by crystallization of glass under the action of catalyst or nucleating agent. Ceramization and vitrification could be mainly used to enhance the stability of electrolyte to better resist the effects of harsh environments and simplify the battery packaging process.

In recent years, chalcogenide glass-ceramic electrolytes have made great progress, such as $Na_{10}GeP_2S_{12}$ glass ceramic (1.2×10^{-5} S cm^{-1}, RT) (Tsuji et al., 2018), $94Na_3PS_4 \cdot 6Na_4SiS_4$ glass ceramic (7.4×10^{-4} S cm^{-1}, RT) (Tanibata et al., 2014b), and AgX (X = S/I)-GeS_2-Sb_2S_3 glass (3.53×10^{-4} S cm^{-1}, RT) (Ma et al., 2020). Recently, Kim et al. reported a layered chalcogenide compound of composition $Na_2(Ga_{0.1}Ge_{0.9})_2Se_{4.95}$ with high room-temperature ionic conductivity (>10^{-5} S cm^{-1}), synthesized as a glass-ceramic composite in the ternary system Na_2Se-Ga_2Se_3-$GeSe_2$ (Kim et al., 2014), as shown in **Figure 2**. Alkali ions containing crystalline chalcogenides are usually hygroscopic and unstable in the environment. The crystalline phase could be stabilized by inserting the glass matrix and forming a three-dimensional continuous percolation network for rapid sodium ion conduction. The results illustrate that the layered chalcogenides with the planar alkali ion diffusion path can be used as a feasible substitute for traditional solid electrolytes.

CONCLUSIONS AND PERSPECTIVE

In conclusion, ion doping and substitution can raise ionic conductivity of the CSEs. However, its effect on the structure stability needs to be further analyzed. Generally, the FPCs can be used to calculate the phonon spectrum, binding energy, and infrared spectrum of the modified materials, so as to

determine the structural stability of the material, and then the experiments of ion doping and substitution could be carried out. The composite method can be widely used to reinforce interface contact. In addition, ceramization and vitrification are also common methods to modify the CSEs, which can improve the ionic conductivity and stability and better resist the influence of a harsh environment. In short, for different electrolytes, it is still necessary to choose appropriate modification methods according to the actual requirement, so as to better augment the performance of electrolytes.

Ultimately, the development of solid-state electrolytes of chalcogenides still faces some challenges, which are summarized as follows:

(1) The CSEs are sensitive to air. In a high-humidity environment, they are easy to deliquesce and release toxic H_2S gas, and they are easy to be oxidized in dry air. Hence, it brings difficulties to the packaging and application of the CSEs.

(2) S or Se in the CSEs is easy to exchange anion with O in oxide anode, and P/Sb/Sn/Ge is easy to be reduced by Na; hence, the interface stability between the electrolyte and the electrode needs to be enhanced.

(3) Although the conductivity of $Na_{10}GeP_2S_{12}$ and $Na_7P_3M_{11}$ (M = O, S, Se) electrolytes is high, it is difficult to synthesize them in the pure phase.

In terms of the above problems, we put forward some suggestions as follows:

(1) The theoretical calculation of element doping and surface coating is carried out by the FPCs to improve the efficiency of the experiments.

(2) Coating the CSEs with an oxide-protective layer or compounding with polymer enhances air stability.

(3) The core–shell structure is designed to limit the decomposition of sulfide during volume expansion.

(4) Combined with the phase diagram, the cooling rate is precisely controlled in the process of melting quenching to obtain the electrolyte with excellent performance.

AUTHOR CONTRIBUTIONS

HD conceived the idea and designed this review. WX collected the related literature resources (with assistance from ZH, YC, XW, BY, ZC, JG, and DY). HD and WX contributed to data analysis and interpretation. WW (with assistance from FX, WZ, RG, and GZ) revised the manuscript. HD wrote the paper. All authors provided feedback.

ACKNOWLEDGMENTS

Financial support from the National Natural Science Foundation of China (No. 61675049) and outstanding doctoral research promotion program of Fudan University (SSH6281011/003) is gratefully acknowledged.

REFERENCES

Bo, S. H., Wang, Y., Kim, J. C., Richards, W. D., and Ceder, G. (2016). Computational and experimental investigations of Na-ion conduction in cubic Na_3PSe_4. *Chem. Mater.* 28, 252–258. doi: 10.1021/acs.chemmater.5b04013

Dai, H., Xu, W., Chen, Y., Li, M., Chen, Z., Yang, B., et al. (2020). Narrow band-gap cathode $Fe_3(PO_4)_2$ for sodium-ion battery with enhanced sodium storage. *Colloids Surf. A* 591, 124561. doi: 10.1016/j.colsurfa.2020.124561

De Klerk, N. J., and Wagemaker, M. (2016). Diffusion mechanism of the sodium-ion solid electrolyte Na_3PS_4 and potential improvements of halogen doping. *Chem. Mater.* 28, 3122–3130. doi: 10.1021/acs.chemmater.6b00698

Hayashi, A., Noi, K., Sakuda, A., and Tatsumisago, M. (2012). Superionic glass-ceramic electrolytes for room-temperature rechargeable sodium batteries. *Nat. Commun.* 3, 1–5. doi: 10.1038/ncomms1843

Hou, W., Guo, X., Shen, X., Amine, K., Yu, H., and Lu, J. (2018). Solid electrolytes and interfaces in all-solid-state sodium batteries: progress and perspective. *Nano Energy* 52, 279–291. doi: 10.1016/j.nanoen.2018.07.036

Kato, Y., Hori, S., Saito, T., Suzuki, K., Hirayama, M., Mitsui, A., et al. (2016). High-power all-solid-state batteries using sulfide superionic conductors. *Nat. Energy* 1, 1–7. doi: 10.1038/nenergy.2016.30

Kim, S. K., Mao, A., Sen, S., and Kim, S. (2014). Fast Na-ion conduction in a chalcogenide glass-ceramic in the ternary system Na_2Se–Ga_2Se_3-$GeSe_2$. *Chem. Mater.* 26, 5695–5699. doi: 10.1021/cm502542p

Kobayashi, T., Chen, F., Seznec, V., and Masquelier, C. (2020). HBO_2 as an adhesive agent for the multi-step fabrication of all-solid-state sodium batteries. *J. Power Sources.* 450:227597. doi: 10.1016/j.jpowsour.2019.227597

Krauskopf, T., Culver, S. P., and Zeier, W. G. (2018a). Local tetragonal structure of the cubic superionic conductor Na_3PS_4. *Inorg. Chem.* 57, 4739–4744. doi: 10.1021/acs.inorgchem.8b00458

Krauskopf, T., Muy, S., Culver, S. P., Ohno, S., Delaire, O., Shao-Horn, Y., et al. (2018b). Comparing the descriptors for investigating the influence of lattice dynamics on ionic transport using the superionic conductor $Na_3PS_{4-x}Se_x$. *J. Am. Chem. Soc.* 140, 14464–14473. doi: 10.1021/jacs.8b09340

Krauskopf, T., Pompe, C., Kraft, M. A., and Zeier, W. G. (2017). Influence of lattice dynamics on Na^+ transport in the solid electrolyte $Na_3PS_{4-x}Se_x$. *Chem. Mater.* 29, 8859–8869. doi: 10.1021/acs.chemmater.7b03474

Luo, W., Calas, A., Tang, C., Li, F., and Mai, L. (2016). Ultralong Sb_2Se_3 nanowire based free-standing membrane anode for lithium/sodium ion batteries. *ACS Appl. Mater. Interfaces* 8:35219. doi: 10.1021/acsami.6b11544

Ma, B., Jiao, Q., Zhang, Y., Sun, X., Yin, G., Zhang, X., et al. (2020). Physical and electrochemical behaviors of AgX (X= S/I) in a GeS_2-Sb_2S_3 chalcogenide-glass matrix. *Ceram. Int.* 46, 6544–6549. doi: 10.1016/j.ceramint.2019.11.138

Mahmoud, M. M. A., Joubert, D. P., and Molepo, M. P. (2019). Structural, stability and thermoelectric properties for the monoclinic phase of $NaSbS_2$ and $NaSbSe_2$: a theoretical investigation. *Eur. Phys. J. B* 92:214. doi: 10.1140/epjb/e2019-90712-y

Noi, K., Nagata, Y., Hakari, T., Suzuki, K., Yubuchi, S., Ito, Y., et al. (2018). Oxide-based composite electrolytes using $Na_3Zr_2Si_2PO_{12}$/Na_3PS_4 interfacial ion transfer. *ACS Appl. Mater. Interfaces* 10, 19605–19614. doi: 10.1021/acsami.8b02427

Park, K. H., Kim, D. H., Kwak, H., Jung, S. H., Lee, H. J., Banerjee, A., et al. (2018). Solution-derived glass-ceramic NaI·Na_3SbS_4 superionic conductors for all-solid-state Na-ion batteries. *J. Mater. Chem. A* 6, 17192–17200. doi: 10.1039/C8TA05537H

Rao, R. P., Chen, H., Wong, L. L., and Adams, S. (2017). $Na_{3+x}M_xP_{1-x}S_4$ (M=Ge^{4+}, Ti^{4+}, Sn^{4+}) enables high rate all-solid-state Na-ion batteries $Na_{2+2\delta}Fe_{2-\delta}(SO_4)_3$|$Na_{3+x}M_xP_{1-x}S_4$|$Na_2Ti_3O_7$. *J. Mater. Chem. A* 5, 3377–3388. doi: 10.1039/C6TA09809F

Richards, W. D., Tsujimura, T., Miara, L. J., Wang, Y., Kim, J. C., Ong, S. P., et al. (2016). Design and synthesis of the superionic conductor $Na_{10}SnP_2S_{12}$. *Nat. Commun* 7:11009. doi: 10.1038/ncomms11009

Takeuchi, S., Suzuki, K., Hirayama, M., and Kanno, R. (2018). Sodium superionic conduction in tetragonal Na_3PS_4. *J. Solid State Chem.* 265, 353–358. doi: 10.1016/j.jssc.2018.06.023

Tanibata, N., Deguchi, M., Hayashi, A., and Tatsumisago, M. (2017). All-solid-state Na/S batteries with a Na_3PS_4 electrolyte operating at room temperature. *Chem. Mater.* 29, 5232–5238. doi: 10.1021/acs.chemmater.7b01116

Tanibata, N., Noi, K., Hayashi, A., Kitamura, N., Idemoto, Y., and Tatsumisago, M. (2014b). X-ray crystal structure analysis of sodium-ion conductivity in $94Na_3PS_4 \cdot 6Na_4SiS_4$ glass-ceramic electrolytes. *ChemElectroChem* 1, 1130–1132. doi: 10.1002/celc.201402016

Tanibata, N., Noi, K., Hayashi, A., and Tatsumisago, M. (2014a). Preparation and characterization of highly sodium ion conducting Na_3PS_4-Na_4SiS_4 solid electrolytes. *RSC Adv.* 4, 17120–17123. doi: 10.1039/C4RA00996G

Tsuji, F., Tanibata, N., Sakuda, A., Hayashi, A., and Tatsumisago, M. (2018). Preparation of sodium ion conductive $Na_{10}GeP_2S_{12}$ glass-ceramic electrolytes. *Chem. Lett.* 47, 13–15. doi: 10.1246/cl.170836

Uematsu, M., Yubuchi, S., Tsuji, F., Sakuda, A., Hayashi, A., and Tatsumisago, M. (2019). Suspension synthesis of $Na_{3-x}PS_{4-x}Cl_x$ solid electrolytes. *J. Power Sources* 428, 131–135. doi: 10.1016/j.jpowsour.2019.04.069

Wan, H., Cai, L., Weng, W., Mwizerwa, J. P., Yang, J., and Yao, X. (2020). Cobalt-doped pyrite for $Na_{11}Sn_2SbS_{11.5}Se_{0.5}$ electrolyte based all-solid-state sodium battery with enhanced capacity. *J. Power Sources* 449:227515. doi: 10.1016/j.jpowsour.2019.227515

Wan, H., Mwizerwa, J. P., Han, F., Weng, W., Yang, J., Wang, C., et al. (2019). Grain-boundary-resistance-less $Na_3SbS_{4-x}Se_x$ solid electrolytes for all-solid-state sodium batteries. *Nano Energy* 66:104109. doi: 10.1016/j.nanoen.2019.104109

Wang, H., Chen, Y., Hood, Z. D., Sahu, G., Pandian, A. S., Keum, J. K., et al. (2016). An air-stable Na_3SbS_4 superionic conductor prepared by a rapid and economic synthetic procedure. *Angew. Chem. Int. Ed.* 55, 8551–8555. doi: 10.1002/anie.201601546

Wang, Y., Richards, W. D., Bo, S. H., Miara, L. J., and Ceder, G. (2017). Computational prediction and evaluation of solid-state sodium superionic conductors $Na_7P_3X_{11}$ (X= O, S, Se). *Chem. Mater.* 29, 7475–7482. doi: 10.1021/acs.chemmater.7b02476

Wang, Y., Song, S., Xu, C., Hu, N., Molenda, J., and Lu, L. (2019a). Development of solid-state electrolytes for sodium-ion battery–A short review. *Nano Mater. Sci.* 1, 91–100. doi: 10.1016/j.nanoms.2019.02.007

Wang, Y., Yang, N., Shuai, Y., Zhang, Y., and Chen, K. (2019b). *Low-Cost Raw Materials Synthesized* $Na_{2.9375}PS_{3.9375}Cl_{0.0625}$ *Solid Electrolyte*. Available online at: https://ssrn.com/abstract=3458155

Xu, X., Li, Y., Cheng, J., Hou, G., Nie, X., Ai, Q., et al. (2020). Composite solid electrolyte of Na_3PS_4-PEO for all-solid-state SnS_2/Na batteries with excellent interfacial compatibility between electrolyte and Na metal. *J. Energy Chem.* 41, 73–78. doi: 10.1016/j.jechem.2019.05.003

Yao, Y., Wei, Z., Wang, H., Huang, H., Jiang, Y., Wu, X., et al. (2020). Toward high energy density all solid-state sodium batteries with excellent flexibility. *Adv. Energy Mater.* 10:1903698. doi: 10.1002/aenm.201903698

Yu, Z., Shang, S. L., Seo, J. H., Wang, D., Luo, X., Huang, Q., et al. (2017). Exceptionally high ionic conductivity in $Na_3P_{0.62}As_{0.38}S_4$ with improved moisture stability for solid-state sodium-ion batteries. *Adv. Mater.* 29:1605561. doi: 10.1002/adma.201605561

Yubuchi, S., Ito, A., Masuzawa, N., Sakuda, A., Hayashi, A., and Tatsumisago, M. (2020). Aqueous solution synthesis for Na_3SbS_4-Na_2WS_4 superionic conductors. *J. Mater. Chem. A* 8, 1947–1954. doi: 10.1039/C9TA02246E

Zhang, D., Cao, X., Xu, D., Wang, N., Yu, C., Hu, W., et al. (2018). Synthesis of cubic Na_3SbS_4 solid electrolyte with enhanced ion transport for all-solid-state sodium-ion batteries. *Electrochim. Acta* 259, 100–109. doi: 10.1016/j.electacta.2017.10.173

Zhang, L., Yang, K., Mi, J., Lu, L., Zhao, L., Wang, L., et al. (2015). Na_3PSe_4: A novel chalcogenide solid electrolyte with high ionic conductivity. *Adv. Energy Mater.* 5:1501294. doi: 10.1002/aenm.201501294

Zhang, L., Zhang, D., Yang, K., Yan, X., Wang, L., Mi, J., et al. (2016). Vacancy-Contained tetragonal Na_3SbS_4 superionic conductor. *Adv. Sci.* 3:1600089. doi: 10.1002/advs.201600089

Zhang, Q., Zhang, C., Hood, Z. D., Chi, M., Liang, C., Jalarvo, N. H., et al. (2020). Abnormally low activation energy in cubic Na_3SbS_4 superionic conductors. *Chem. Mater.* 32, 2264–2271. doi: 10.1021/acs.chemmater.9b03879

Zhao, C., Liu, L., Qi, X., Lu, Y., Wu, F., Zhao, J., et al. (2018). Solid-state sodium batteries. *Adv. Energy Mater.* 8:1703012. doi: 10.1002/aenm.201703012

Zhong, J., He, L., Li, C., Cao, Y., Wang, J., Fang, B., et al. (2014). Coordinated control for large-scale EV charging facilities and energy storage devices participating in frequency regulation. *Appl. Energy* 123, 253–262. doi: 10.1016/j.apenergy.2014.02.074

Zhu, Z., Chu, I. H., Deng, Z., and Ong, S. P. (2015). Role of Na^+ interstitials and dopants in enhancing the Na^+ conductivity of the cubic Na_3PS_4 superionic conductor. *Chem. Mater.* 27, 8318–8325. doi: 10.1021/acs.chemmater.5b03656

Conflict of Interest: The authors declare that the research was conducted in the absence of any commercial or financial relationships that could be construed as a potential conflict of interest.